BIOCHEMISTRY
including biophysical chemistry & molecular biology

ARTICLE

pubs.acs.org/biochemistry

Spectroscopic Evidence for the Formation of an N Intermediate during the Photocycle of Sensory Rhodopsin II (Phoborhodopsin) from *Natronobacterium pharaonis*

Yusuke Tateishi,[†] Takayuki Abe,[‡] Jun Tamogami,[‡,∥] Yutaka Nakao,[‡] Takashi Kikukawa,[§] Naoki Kamo,[*,∥] and Masashi Unno[*,†,⊥]

[†]Department of Chemistry and Applied Chemistry, Graduate School of Science and Engineering, Saga University, Saga 840-8502, Japan

[‡]Faculty of Advanced Life Science and Graduate School of Pharmaceutical Sciences, Hokkaido University, Sapporo 060-0810, Japan

[§]Graduate School of Science, Hokkaido University, Sapporo 060-0810, Japan

[∥]College of Pharmaceutical Sciences, Matsuyama University, Bunkyo-cho, Matsuyama 790-8578, Japan

[⊥]PRESTO, JST, 4-1-8 Honcho, Kawaguchi, Saitama 332-0012, Japan

Supporting Information

ABSTRACT: Sensory rhodopsin II is a seven transmembrane helical retinal protein and functions as a photoreceptor protein in negative phototaxis of halophilic archaea. Sensory rhodopsin II from *Natronomonas pharaonis* (NpSRII) is stable under various conditions and can be expressed functionally in *Escherichia coli* cell membranes. Rhodopsins from microorganisms, known as microbial rhodopsins, exhibit a photocycle, and light irradiation of these molecules leads to a high-energy intermediate, which relaxes thermally to the original pigment after passing through several intermediates. For bacteriorhodopsin (BR), a light-driven proton pump, the photocycle is established as BR → K → L → M → N → O → BR. The photocycle of NpSRII is similar to that of BR except for N, i.e., M thermally decays into the O, and N has not been well characterized in the photocycle. Thus we here examined the second half of the photocycle in NpSRII, and in the present transient absorption study we found the formation of a new photointermediate whose absorption maximum is ∼500 nm. This intermediate becomes pronounced in the presence of azide, which accelerates the decay of M. Transient resonance Raman spectroscopy was further applied to demonstrate that this intermediate contains a 13-*cis* retinal protonated Schiff base. However, detailed analysis of the transient absorption data indicated that M-decay does not directly produce N but rather produces O that is in equilibrium with N. These observations allowed us to propose a structural model for a photocycle that involves N.

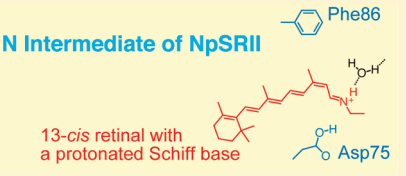

Understanding protein function at the atomic level is a major challenge in the field of biological chemistry and requires the combined use of structural and functional methods. We have previously used photoreceptor proteins as model systems to understand in atomic detail how a chromophore and a protein interact to sense light and send a biological signal. Sensory rhodopsin II (also called phoborhodopsin) from *Natronobacterium pharaonis* (NpSRII) functions as a photophobic receptor that enables bacteria to avoid damaging photo-oxidative conditions.[1−3] This seven helical membrane protein belongs to the family of microbial rhodopsins, which was first identified in *Halobacterium salinarum*. Representatives of this protein family include the light activated ion pumps bacteriorhodopsin (BR) and halorhodopsin as well as two phototaxis receptors, sensory rhodopsin I (SRI) and II (SRII).[4] Microbial rhodopsins have several common features, including an all-*trans*-retinylidene chromophore covalently attached to the protein via a protonated Schiff base linkage. Light absorption results in an all-*trans* → 13-*cis*-isomerization of the chromophore that triggers subsequent conformational changes associated with a photocycle characteristic of each protein.[4] In the case of the photocycle for BR,[5] the photoisomerization leads to the formation of early intermediates (K and L), and a transition to an M intermediate involves a proton transfer from the protonated Schiff base to Asp85, a counterion of the protonated Schiff base. The Schiff base is then reprotonated by proton-donating groups of Asp96 and Thr46 located on the cytoplasmic side to form an N intermediate. The isomerization of the retinal chromophore back to the all-*trans* form produces an O intermediate, which then returns to its original BR state.

The photocycle of NpSRII has intermediates analogous to BR. There are, however, key differences between the two proteins. First, the M intermediate of NpSRII decays to O in about 1 s,[6,7] which is substantially slower compared to the 5 ms decay of M in BR.[5] In the course of the M to O transition in NpSRII, the deprotonated Schiff base takes up a proton from the external media.[8] Because of the lack of proton-donating groups in NpSRII (Asp96 and Thr46 in BR correspond to Phe86 and Leu40 in

Received: December 8, 2010
Revised: February 1, 2011
Published: February 07, 2011

NpSRII, respectively), the reprotonation of the Schiff base is significantly slow.[9] The long-lived M and O are considered to be important in the interaction with the transducer.[1] Another difference between NpSRII and BR is related to the N intermediate. In an initial transient absorption study on NpSRII on a millisecond time scale, N was not observed during the M to O transition.[6] Subsequently, Chizhov et al.[7] performed a global fitting analysis of transient absorption data under various conditions. Although the presence of N was not obvious in the raw data, the analysis suggested the formation of N as an equilibrium state with the more pronounced M and O intermediates. Thus, N is still poorly characterized; as a typical example, FTIR studies did not detect spectral features characteristic to N in BR.[10,11]

As described above, the existence of N is unsure at present. Moreover, even if N exists, its fraction during the photocycle must be small. One possible explanation for why N would be present in a small fraction would be the long lifetime of M. That is, when the lifetime of M is longer than that of N, the relatively short-lived N will not populate in an observable amount. We may therefore expect that N populates in an observable amount, when the decay of M is accelerated. A possible method for accelerating the decay of M would be the addition of azide. Takao et al.[12] have shown that azide increases the reprotonation rate of the Schiff base, which causes an acceleration of the M decay. Analogously, lowering the pH also shortens the lifetime of M.[6]

Thus, in the present study, we apply transient absorption as well as resonance Raman spectroscopy to NpSRII in the presence or absence of azide to obtain information concerning the molecular mechanism of the photocycle of NpSRII. We also examine the effects of pH on its photocycle. Transient absorption spectroscopy in the ultraviolet−visible region is a powerful technique to investigate the impact of azide or lowering pH on the kinetics for the photocycle. On the other hand, vibrational spectroscopy such as Raman scattering is ideally suited to examining the molecular structures of the transient species. In particular, the vibrational spectra of specific intermediate states can be selected by tuning the laser wavelength in the resonance Raman technique. Using both transient absorption and resonance Raman spectroscopy, we present spectroscopic evidence that demonstrates the presence of N, which is in equilibrium with O. The present findings provide important information concerning the decay process of M, which is considered to be a signaling state of this photoreceptor protein.[1]

MATERIALS AND METHODS

Sample Preparations. The expression and purification of histidine-tagged recombinant NpSRII were conducted as previously described.[13] Briefly, NpSRII possessing a histidine tag at the C-terminus was expressed in *Escherichia coli*, solubilized with 1.0% *n*-dodecyl-*β*-D-maltoside (DDM), and purified with an Ni-column. The buffer solution used in the spectroscopic measurements was 10 mM six-mixed buffer (citric acid, MES, HEPES, MOPS, CHES, and CAPS at 10 mM each) containing 400 mM NaCl and 0.1% DDM.

Transient Absorption Spectroscopy. All measurements were performed at 20 °C. The details of the transient absorption apparatus and the procedure for data analysis were reported previously.[14] The transient absorption changes induced by a laser pulse (Nd:YAG, 532 nm, 7 ns, 5 mJ/pulse) were acquired in a computer. The data before the laser pulse were adopted as a baseline for calculation of the subsequent absorption change. At each selected measuring wavelength (every 10 nm from 300 to 650 nm), 5−20 laser pulses were used to improve the signal-to-noise ratio. The data points were then selected by choosing a logarithmic time scale to reduce the number of points.

Data Analysis of Photocycling. The data observed at all wavelengths from 300 to 650 nm were fitted simultaneously with the following multiexponential equation:

$$\Delta A(\lambda, t) = \sum_{i=1}^{n} B_i(\lambda) \exp(-t/\tau_i) \quad (1)$$

For each data set, the fittings were performed using 3−5 exponential functions, and the reductions in the standard deviation of the weighted residuals were saturated with $n = 3$ or 4. Here, τ_i of eq 1 represents the decay time constant of the ith component that is expressed as P_i, the photochemically defined intermediate, according to Chizhov et al.[15]

$$P_0(\text{NpSRII}) \rightarrow P_1 \xrightarrow{\tau_1} P_2 \xrightarrow{\tau_2} \quad \ldots \quad P_i \xrightarrow{\tau_i} P_0 \quad (2)$$

The P_i is permitted to be a mixture of physically defined photointermediates. The $B_i(\lambda)$ term in eq 1 is formulated as

$$B_i(\lambda) = F_C \sum_{j=1}^{n} a_{ij} \Delta\varepsilon_j(\lambda) \quad (i = 1, 2, \quad \ldots \quad n) \quad (3)$$

where

$$a_{ij} = 1/\left(\prod_{m=1}^{j-1} \tau_m \prod_{\substack{m=1 \\ m \neq i}}^{j} (1/\tau_m - 1/\tau_i) \right)$$

and $\Delta\varepsilon_j(\lambda)$ stands for the absorption difference between P_i and P_0 (NpSRII) at wavelength λ when all P_0 (NpSRII) molecules in the cuvette are photolyzed. F_C is the fraction of the P_0 molecule that is activated by the flash to undergo the photocycle. Equation 3 indicates that the B spectra of the last component ($i = n$) are given by

$$B_n(\lambda) = F_C a_{nn} \Delta\varepsilon_n(\lambda), a_{nn} = 1/\left(\prod_{m=1}^{n-1} (1 - \tau_m/\tau_n) \right)$$

meaning that $F_C\Delta\varepsilon_n(\lambda)$ can be determined from $B_n(\lambda)$, which is already known from the fitting with eq 1. Once $F_C\Delta\varepsilon_n(\lambda)$ of the nth component is determined, $F_C\Delta\varepsilon_{n-1}(\lambda)$ of the $(n-1)$th component can be easily determined using eq 3. Then, we can determine $F_C\Delta\varepsilon_i(\lambda)$ for all components iteratively under an appropriate order of time constants (τ_1, τ_2, ..., τ_n) in the photocycle. The negative part of $F_C\Delta\varepsilon_i(\lambda)$ originates from the depletion of P_0 by the flash excitation. Thus the criterion for determining the order is the absence of a negative part except for the P_0 absorption band. Then, we examined all possible sequences of the order for the calculation of $F_C\Delta\varepsilon_i(\lambda)$, and the best sequence was chosen. In the present case, a unique choice was obtained. Finally, the addition of the F_C times spectrum of the original NpSRII gives the spectrum of P_i. The value of F_C was determined so that the evaluated spectra, composed of mainly a single physically defined intermediate, would conform to the skewed Gaussian function.[16]

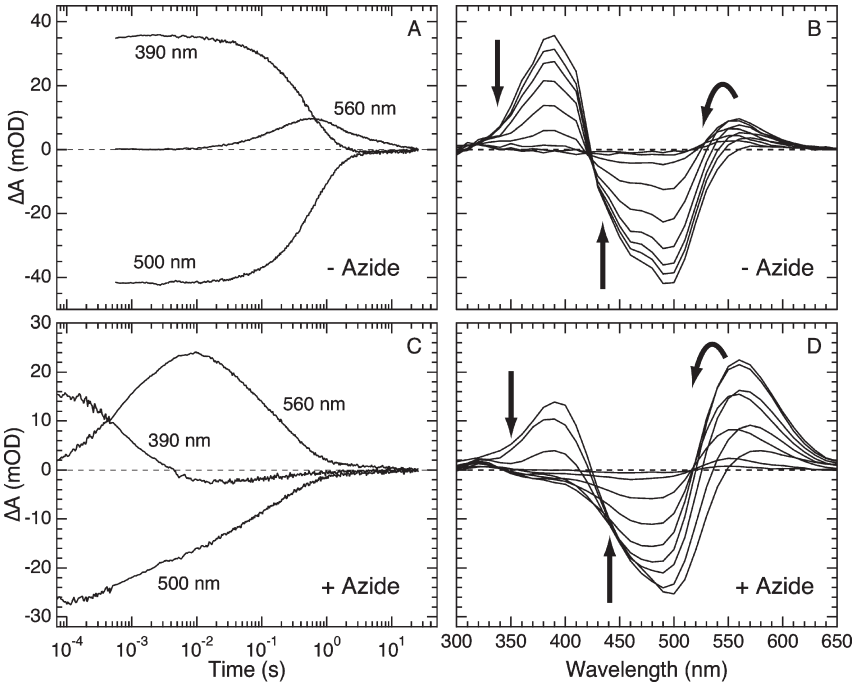

Figure 1. Transient flash-induced absorption changes of NpSRII in the absence (A, B) or presence (C, D) of 200 mM NaN_3. Measurements were performed at 20 °C in solutions of 10 mM six-mix buffer (citrate, MES, HEPES, MOPS, CHES, and CAPS), 400 mM NaCl, and 0.1% DDM at pH 6.5 (A, B) or pH 6.0 (C, D). The kinetic traces were monitored at 390, 500, and 560 nm. (B) The difference spectra at 1.2, 68.9, 131, 251, 477, and 910 ms and at 1.73, 3.30, and 6.30 s after illumination. (D) The difference spectra at 0.097, 0.35, 1.3, 5.2, 19.0, 69.0, 251, 910, and 3300 ms after illumination.

Resonance Raman Spectroscopy. The resonance Raman spectra were obtained as described earlier.[17] The spectrometer system was composed of a helium−cadmium laser (IK5651R-G; Kimmon Electric Ltd., Tokyo, Japan) or a semiconductor solid-state green laser (Ventus532-1500, LaserQuantum, Cheshire, U. K.), a 0.5 m single spectrometer (Spex 500M, HORIBA Jobin Yvon, Edison, NJ) equipped with a 1800 groove/mm holographic grating, and a liquid nitrogen-cooled UV-coated CCD detector (Spec-10:400B; Roper Scientific Inc., Trenton, NJ). The 441.6 nm line from the helium−cadmium laser was mainly used to measure the resonance Raman spectra. A 90° scattering geometry was employed, and the scattered photons were collected and focused onto the entrance slit of a spectrometer by using two quartz plano-convex lenses. A polarization scrambler was placed at the entrance slit to remove the effects of polarization from the spectrometer throughput. A Triax190 spectrometer (HORIBA Jobin Yvon, Edison, NJ) was used to remove the excitation light, and the first order of the dispersed light by the 500M spectrometer was imaged on the detector. An entrance slit width of 0.1 mm corresponded to a spectral resolution of ~4 cm^{-1}. All spectra were taken at room temperature (~25 °C), and homemade software was used to eliminate the noise spikes in the spectra caused by cosmic rays. All Raman spectra were calibrated by using neat fenchone as a standard. Sample volumes were 50 μL and were contained in a quartz spinning cell (10 mm in diameter). The cell was spun at 1600 rpm. Most of the resonance Raman spectra for the dark and intermediate states excited at 441.6 nm were obtained by a single-beam method (see Figure 1S in the Supporting Information),[18] and the transit time of the sample in the beam was ~40 μs. We performed the measurement of NpSRII with a low laser power (0.1 mW; photoalteration parameter[18] $F = 0.096$), while a higher laser power (1.0 mW; $F = 0.96$ or 2.5 mW; $F = 2.4$) was used for the intermediate states. In some experiments, we also used a dual-beam apparatus where the pump beam was spatially displaced from the probe beam (Figure 1S, panel B in the Supporting Information) to avoid a contamination of short-lived intermediates such as L (lifetime, ~30 μs).[7] In this arrangement, transient resonance Raman spectra of intermediate states whose lifetime is longer than ~30 ms were detected.

RESULTS

Effects of Azide and Lowering pH on the Photocycle of NpSRII. Figure 1A shows time-traces for the absorbance changes of NpSRII at the three diagnostic wavelengths, 390, 500, and 560 nm. Note the logarithmic time scale ranging from 70 μs to 50 s. The depletion signal at 500 nm reflects the initial amount of bleach due to the formation of M. The signal at 390 nm primarily corresponds to the initial formation and decay of M, while the signal at 560 nm is mainly due to the formation and decay of O. Figure 1B displays the flash-induced light-dark difference spectra between 300 and 650 nm. The negative band around 500 nm is due to the depletion of the original NpSRII. The positive bands at 390 and 550 nm are assigned to M and O, respectively. These results are consistent with previous transient absorption studies of NpSRII.[6,7] Figure 1C,D demonstrates the impact of the addition of azide to the photocycle of NpSRII. The decay of M as well as the formation of O are accelerated to ~1 ms in the presence of 200 mM NaN_3. Moreover, the amount of O formed was significantly increased in the presence of azide. Because M decay is associated with the entry of the proton from the medium, lowering the pH also accelerates the decay of M.[6] Figure 2S in the Supporting Information illustrates the transient absorption data of NpSRII at pH 3.5. A comparison of Figure 1 and Figure 2S in the Supporting Information demonstrates that the decay of M is

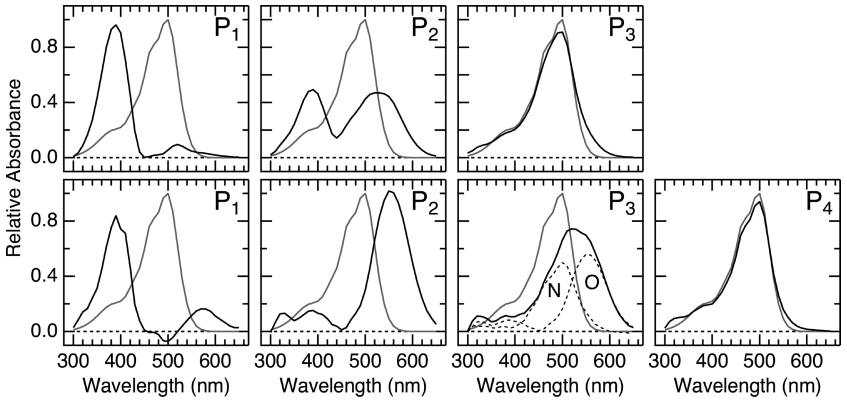

Figure 2. Spectra of intermediates obtained by global fitting analysis of the transient absorption data of NpSRII. (Upper panels) NpSRII in the absence of NaN_3. (Lower panels) NpSRII in the presence of 200 mM NaN_3. The gray lines represent the spectrum of P_0. The spectrum of P_3 for NpSRII with azide is composed of two physically different intermediates, and the dotted lines show the spectra of the components. The estimated time constants are τ_1 = 312 ms, τ_2 = 597 ms, and τ_3 = 7230 ms for data in the absence of azide, and τ_1 = 1.28 ms, τ_2 = 45.4 ms, τ_3 = 284 ms, and τ_4 = 4940 ms for data in the presence of azide. The media were 400 mM NaCl and 0.1% DDM containing 10 mM six-mix buffer at pH 6.5 (upper panels) or 6.0 (lower panels).

accelerated concomitant with an increase in the fraction of O at lower pH. Figure 3S in the Supporting Information summarizes the effects of azide and pH on the decay process of M.

The data observed at all wavelengths from 300 to 650 nm were fitted simultaneously with mutiexponential eq 1. The addition of azide increased the number of exponential terms from three to four to obtain satisfactory fits. These data were further analyzed as described in the Materials and Methods, and Figure 2 shows the results of this analysis. The upper panels exhibit the calculated spectra P_i of NpSRII in the absence of azide in the order of their appearance after the flash. P_1 exhibits an absorption maximum at 390 nm and is assigned to M.[6,7] The spectrum of P_2 shows two absorption maxima, indicating that P_2 consists of at least two physically defined intermediates that attain equilibrium at a rate much faster than the rate of decay. The absorption maximum of the short wavelength component is 390 nm, and thus was due to M. The absorption spectrum for the second component of P_2 is centered at 530 nm. Although this component can be related to O, its absorption maximum is blue-shifted by ~30 nm compared to the reported value of 560 nm.[6,7] Furthermore, this absorption band centered at 530 nm is significantly broad, suggesting the presence of an additional intermediate whose absorption maximum was around 500 nm. P_3 has the longest lifetime of all intermediates. Its absorption spectrum is quite similar to that of the initial dark state NpSRII (P_0), and a similar intermediate was previously detected.[7] This species probably contains an all-*trans*-retinylidene chromophore with a protonated Schiff base like the initial NpSRII, although the protein structure may not be fully relaxed. In this paper, we denote this 500 nm species as NpSRII′. We also performed a global fitting analysis for NpSRII at pH 3.5 (Figure 2S in the Supporting Information). This analysis, however, failed to provide physically relevant spectra P_i. At lower pH, a counterion Asp75 of the protonated Schiff base of the chromophore is protonated (pK_a = 3.5).[19] Thus Asp75 in NpSRII at pH 3.5 is a mixture of protonated and deprotonated forms, and this sample heterogeneity probably makes the sequential photocycle model (eq 2) inadequate.

The lower panels of Figure 2 display the spectra P_i for NpSRII in the presence of 200 mM NaN_3. To demonstrate that the result shown in Figure 2 is a unique solution of the analysis, supplemental data are given as Figure 4S in the Supporting Information. The absorption spectrum of P_1 for NpSRII with azide closely resembles that for NpSRII without azide and is ascribed to M. The addition of azide significantly affects the spectrum of P_2, which exhibits an absorption maximum around 560 nm. This 560 nm component is assigned to O.[6,7] The spectrum of P_3 is centered near 530 nm, and this broad absorption band can be correlated to the 530 nm band of P_2 for NpSRII without azide (see Figure 5S in the Supporting Information). The long-lived P_4 corresponds to P_3 for NpSRII without azide. The results for NpSRII with azide shown in Figure 2 indicate that the decay of M (P_1) leads to the formation of O (P_2). The next component P_3 has an absorption band around 530 nm. Since this absorption band is significantly broad, as indicated above, two intermediates could contribute to the spectrum. Thus we performed a spectral analysis by assuming that one of the components for P_3 is O. The results shown in Figure 2 (P_3 in the lower panels) demonstrate that the broad absorption band for P_3 can be explained as the sum of the spectrum of P_2 multiplied with a factor of 0.45 and a spectrum centered around 500 nm. In the case of BR, the absorption maximum of N (560 nm) is close to that of the light-adapted state BR (568 nm).[5] We therefore suggest that the 500 nm component of P_3 is N. To confirm this assignment, we next performed resonance Raman investigations and examined the formation of N, which contains a 13-*cis*-retinylidene chromophore with a protonated Schiff base.

Resonance Raman Spectra of NpSRII. Figure 3 depicts the resonance Raman spectra of the dark and intermediate states with 441.6 nm excitation. The spectra of NpSRII in H_2O (trace a) and D_2O (trace b) are consistent with previous works.[20,21] The most prominent feature is the ethylenic stretch $\nu_{C=C}$ observed at 1548 cm^{-1}. As illustrated in Figure 4, an approximately linear correlation exists between the absorption maximum (λ_{max}) of retinal compounds and the ethylenic stretching frequency $\nu_{C=C}$.[22] In NpSRII, the 1548 cm^{-1} frequency of $\nu_{C=C}$ corresponds to a λ_{max} of ~490 nm, which is in reasonable agreement with the measured absorption maximum of ~500 nm. The Raman band at 1652 and 1347 cm^{-1} is assigned to the C=N stretching ($\nu_{C=N}$) and N−H bending (δ_{N-H}) modes of a Schiff base linkage to the protein, respectively. These assignments as well as the protonation state of the Schiff base are demonstrated by the sensitivity of these modes to deuteration. A comparison of traces a and b in Figure 3 indicates that the H/D exchange downshifts the $\nu_{C=N}$ band at 1652 cm^{-1} by ~21 cm^{-1}, and the

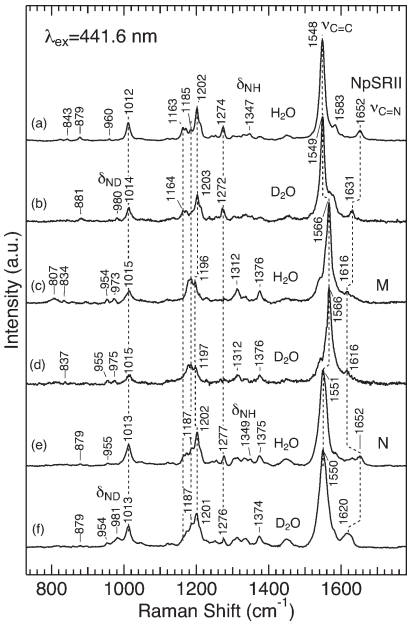

Figure 3. Resonance Raman spectra of dark and photointermediates of NpSRII with 441.6 nm excitation: (a, b) dark state, (c, d) M intermediate, and (e, f) N intermediate. Traces a, c, and e are the spectra in H_2O, whereas traces b, d, and f are the spectra in D_2O. The medium contained 10 mM six-mix buffer, 400 mM NaCl, and 0.1% DDM at pH 7.0.

δ_{N-H} band exhibits a 367 cm^{-1} downshift upon deuteration. For retinals, the C−C skeletal stretching modes in the 1100−1400 cm^{-1} region are called the "fingerprint region" and are sensitive indicators of chromophore geometry.[18] The resonance Raman spectra of NpSRII are characterized by bands at 1202 and 1163 cm^{-1}, and these are indicative of an all-*trans* configuration. The mode at 1202 cm^{-1} is assigned to the C14−C15 stretch, and the C12−C13 stretch is the band at 1163 cm^{-1}.[1,23,24]

The experiments on photointermediate states utilized a same spinning cell apparatus as the experiments on the dark state NpSRII, but the former experiments had a higher incident laser power. Figure 5A presents the results of transient resonance Raman experiments on NpSRII without azide. Trace b is obtained under a low power condition, which gives the spectrum for the dark state as mentioned above. The high power spectrum (trace a) exhibits new bands at 1616, 1566, 1314, 1184, and 973 cm^{-1}, indicating the formation of an intermediate state. Subtraction of the low power spectrum from the high power one to minimize the positive or negative 1652 and 1548 cm^{-1} intensities gives a difference spectrum (trace c). We have performed similar experiments for NpSRII in a deuterated buffer, and the resultant spectra for the H_2O and D_2O samples are compared as traces c and d in Figure 3, respectively. These spectra are characterized by an intense $\nu_{C=C}$ band at 1566 cm^{-1}. Since this $\nu_{C=C}$ frequency corresponds to an absorption maximum around 400 nm (see Figure 4), the observed spectra are mainly ascribed to M. A similar $\nu_{C=C}$ frequency for M was reported by previous resonance Raman experiments of NpSRII with 413 nm excitation.[25] The present resonance Raman spectrum of M exhibits a small band at 1616 cm^{-1}, which is assigned to the $\nu_{C=N}$ mode. As shown in Figure 3, the formation of M causes a 36 cm^{-1} downshift of $\nu_{C=N}$ (trace a → c). A similar large downshift of $\nu_{C=N}$ was also observed for the formation of M in

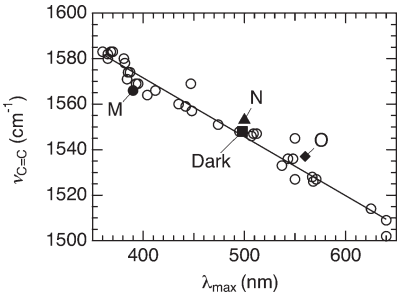

Figure 4. Plot of the observed ethylenic stretching frequency $\nu_{C=C}$ and the absorption maximum λ_{max} of retinal proteins and model compounds. The closed symbols represent data for NpSRII (■), M (●), N (▲), and O (◆). The ○ are data for several retinal proteins and model compounds taken from ref 22.

BR (1640 → 1621 cm^{-1}, see Table 1).[18,24,26] Figure 3 also demonstrates that the $\nu_{C=N}$ band is insensitive to the H/D exchange (trace c → d), implying the deprotonated Schiff base. This confirms that the observed spectra originate from M.

Here we should note the results of the pump and probe measurements using a dual-beam apparatus (Figure 1S, panel B in the Supporting Information), which eliminates a possible contamination of short-lived intermediates such as L. Figure 6S in the Supporting Information shows the results of the pump and probe experiment on NpSRII without azide. Trace b is the probe-only spectrum, which is the spectrum for the dark state. The pump + probe spectrum (trace a) exhibits some new bands, and subtraction of the probe-only spectrum from the pump + probe one provides a difference spectrum (trace c). A comparison between Figure 5 and Figure 6S in the Supporting Information demonstrates that both single-beam and dual-beam experiments give indistinguishable transient resonance Raman spectra of M, implying that a short-lived intermediate such as L contributes little to the spectra reported here.

Another issue that should be mentioned is a possible effect of secondary photoreactions. For example, a photoproduct of a long-lived intermediate might contribute to the transient resonance Raman spectra with a high photoalteration parameter *F*. We can, however, rule out this possibility, because the spectra reported here do not show a band at 1580 cm^{-1}, which was previously ascribed to a photoproduct of M.[25] Further supporting evidence was obtained from an experiment with a lower *F* value of 1.0. Figure 7S in the Supporting Information demonstrates a close similarity between the transient resonance Raman spectra with *F* = 1.0 (trace a) and 2.5 (trace b), implying negligible secondary photoreactions.

Effects of Azide on the Resonance Raman Spectra of NpSRII. Figure 5B displays the results for NpSRII in the presence of 200 mM NaN_3. The addition of azide does not affect the low power spectra (traces b and e), indicating that the active site structure of NpSRII is not influenced by azide. However, the high power spectrum depends on the presence of azide (trace a → d); e.g., a prominent Raman band at 1566 cm^{-1} diminishes intensity upon addition of azide. The transient resonance Raman spectrum was then calculated by subtracting the low-power spectrum from the high-power one, resulting in the spectrum in trace f. It is clear that the transient resonance Raman spectra differ significantly between NpSRII with (trace f) and without azide (trace c), and the spectrum obtained in the presence of azide is characterized by bands at 1652, 1550, 1202,

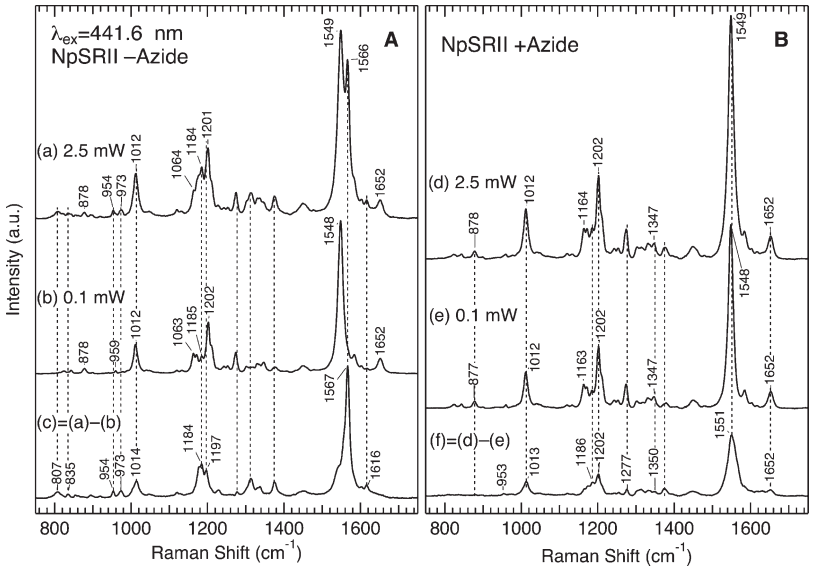

Figure 5. Transient resonance Raman spectra of photointermediates for NpSRII without (A) and with (B) 200 mM NaN_3. The excitation wavelength was 441.6 nm, and the medium was 10 mM six-mix buffer, 400 mM NaCl, and 0.1% DDM at pH 7.0.

Table 1. Vibrational Frequency (cm^{-1}) and Absorption Maximum (nm) of NpSRII, BR, and Their Photointermediates[a]

	$\nu_{C=C}$	$\nu_{C=N}$ (H_2O)	$\nu_{C=N}$ (D_2O)	$\Delta\nu$(H/D)	λ_{max}
NpSRII	1548	1652	1631	−21	498
M^{NpSRII}	1566	1616	1616	0	390
N^{NpSRII}	1550	1652	1620	−32	500
O^{NpSRII} [b]	1540	nd	nd	nd	560
BR[c]	1528	1641	1624	−17	568
M^{BR} [d]	1567	1621			410
N^{BR} [d,e]	1532	1643	1618	−25	560
O^{BR} [f]	1509	1628	1589	−39	640

[a] $\Delta\nu$(H/D) is the D_2O-induced shift of $\nu_{C=N}$. nd = not determined. [b] Reference 21 and this study. [c] Reference 23. [d] Reference 24. [e] Reference 27. [f] Reference 28.

1186, and 1013 cm^{-1}. This spectrum can be ascribed to the 500 nm component of P_3, which we ascribed to N for the following reasons. As we described above, the present transient absorption studies indicate that the addition of azide shortens the lifetime of M. This leads to a decrease in the fraction of M during a photocycle, whereas the fractions of O (λ_{max} = 530 nm) and N (λ_{max} = 500 nm) are increased (Figures 1 and 2). As seen in Figure 2, the probe wavelength of 441.6 nm is suited for the resonance enhancement of N. In addition, the estimated absorption spectrum of O has no absorption at 441.6 nm, implying that it is almost completely out of resonance. It is, therefore, reasonable to assign the transient resonance Raman spectrum obtained in the presence of azide to N. Indeed, the observed $\nu_{C=C}$ frequency of 1550 cm^{-1} correlates well with the estimated absorption maximum of 500 nm (Figure 4). Further evidence confirming the contribution of N is provided by the resonance Raman measurements with 532 nm excitation. As shown in Figure 8S in the Supporting Information, the transient resonance Raman spectra from 532 nm excitation distinctly differ from those obtained with 441.6 nm excitation (Figures 3 and 4). For instance, the 532 nm spectrum (trace c in Figure 8S in the Supporting Information) exhibits a $\nu_{C=C}$ stretching band around 1540 cm^{-1}, which is mainly assignable to O.[20,21] This observation demonstrates that the broad absorption band of P_3 comprises two components, i.e., the short wavelength component N gives the transient resonance Raman spectrum with 441 nm excitation (Figures 3 and 4), whereas the 532 nm spectrum (Figure 8S in the Supporting Information) mainly represents the longer wavelength component O.

We have also obtained the resonance Raman spectra of N in a deuterated buffer, and Figure 3 compares the resulting spectra of N with those of NpSRII and M. As can be seen, the intense $\nu_{C=C}$ band of N around 1550 cm^{-1} is somewhat broader than that of NpSRII or M. In the case of BR, the $\nu_{C=C}$ band for N is also broad, and its main band at 1532 cm^{-1} has a shoulder at 1549 cm^{-1}.[24,27] Although the reason for the broadness is not known,[27] this is a common feature of N between NpSRII and BR. As noted above, the resonance Raman spectrum of N in H_2O exhibits a band at 1652 cm^{-1}, which is assigned to $\nu_{C=N}$. The shift of the $\nu_{C=N}$ band to 1620 cm^{-1} in D_2O is good evidence that N has a protonated Schiff base. The resonance Raman spectrum of N in H_2O shows a small feature at 1349 cm^{-1}, and this band is assigned to δ_{N-H}. This δ_{N-H} band exhibits a large downshift to 981 cm^{-1} upon deuteration, confirming the protonated Schiff base in N. The fingerprint region of the spectra for N is characterized by bands at 1202, 1186, 1174, and 1165 cm^{-1}. Similar Raman bands are also observed for N in BR,[24,27] supporting a 13-*cis*-retinylidene chromophore in N.

Here we note that a signature of N is also observed in the transient resonance Raman spectra of NpSRII without aizde. As discussed above, traces c and d in Figure 3 are mainly ascribed to the spectra of M. However, the intense band at 1566 cm^{-1} has a shoulder around 1550 cm^{-1}, which can be correlated to N. To support this assignment, we have measured the transient resonance Raman spectrum of the Thr204 → Ala (T204A) mutant. Because the T204A mutant exhibits a longer lifetime of M compared to wild-type, we expect little accumulation of N during the photocycle.[29] As expected, Figure 9S in the Supporting Information demonstrates a lack of the shoulder around 1550 cm^{-1} for T204A.

Scheme 1

Scheme 2

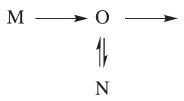

Scheme 3

DISCUSSION

Photocycle of NpSRII: The Presence of an N Intermediate. The photocycle of BR has been well characterized: the primary intermediates thermally decay back to BR through the K, L, M, N, and O intermediates, as shown as Scheme 1, where early intermediates such as K and L are omitted.[4,5] Although the overall photocycle of NpSRII is similar to that of BR, the presence or absence of N was not clear.[6,7,10,11] The present transient absorption study provides spectroscopic evidence showing the formation of an N intermediate with a λ_{max} of ~500 nm. This component becomes pronounced in the presence of azide, which accelerates the decay of M. Moreover, the resonance Raman investigation demonstrates that the 500 nm intermediate contains a 13-*cis*-retinylidene chromophore with a protonated Schiff base linkage. These observations correspond well with the properties of an N-intermediate. There is, however, a clear distinction between BR and NpSRII. The transient absorption data shown in Figure 2 demonstrate that N appears as equilibrium with O after the M to O transition. Thus we suggest a reaction sequence illustrated in Scheme 2 as a photocyle model of NpSRII. A similar photocycle model was also proposed in a new class of sensory rhodopsin III from *Haloarcular marismortui*.[30] We note, however, that although Scheme 2 is a plausible model that accounts for the data shown in Figure 2, a different model such as Scheme 3 cannot be excluded. The determination of a detailed kinetic scheme is important, but it is beyond the scope of this study.

Although Scheme 2 is consistent with the present data, there is a puzzling aspect of the photocycle model; M has a 13-*cis* retinal chromophore and a deprotonated Schiff base, while O has an all-*trans* retinal chromophore and a protonated Schiff base. Thus, two steps proceed during the M → O transition. As illustrated in Scheme 4, it is therefore probable that a *true* N intermediate having a protonated Schiff base with a 13-*cis* retinal chromophore would form after M, but this intermediate is very labile and decays immediately. After the formation of O, structural changes in a protein moiety would take place to accommodate the 13-*cis*-chromophore in N.

Here we note that Chizhov et al.[7] previously suggested the appearance of an intermediate with λ_{max} = 485 nm after the formation of O, and this species was considered to be N. Their results support our photocycle model shown as Scheme 4, although the estimated absorption maximum was slightly

Scheme 4

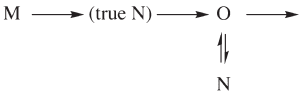

different from ours (500 nm).[a] We should also comment on a previous study that examined the time-resolved FTIR spectra of NpSRII with and without azide.[11] Although a distinct effect of azide on the FTIR spectra was observed, there was no clear indication of the formation of N. This may have been due to the fact that N is only present as equilibrium with more pronounced M and O intermediates. On the other hand, the FTIR study showed the presence of a short-lived intermediate denoted as MO.[11] Because this intermediate is suggested to have a red-shifted absorption maximum, a further resonance Raman study with 532 nm excitation may provide its structural information.

Structure and Spectroscopic Properties of the N Intermediate of NpSRII. The present study reports the transient resonance Raman spectra of N and provides structural information concerning the photocycle of NpSRII. The protonated Schiff base C=N stretching frequency and its frequency shift in D_2O provide important information about interactions at the Schiff base group.[18,31] The frequency shift of the $\nu_{C=N}$ band upon deuteration of the Schiff base nitrogen depends on the strength of its hydrogen bond with the environment, while the frequency of the C=ND stretching mode is an index of the C=N bond order. The correlation between the deuteration shift and the hydrogen bonding strength results from the coupling of the C=N stretching mode with the N−H rocking mode. Deuteration of the nitrogen reduces this coupling as a result of the decreased N−D rocking frequency. A decreased level of hydrogen-bonding interaction with an environmental hydrogen-bond acceptor will lower the N−H rock frequency, causing a lower Schiff base stretch and a reduced deuteration-induced shift.[18]

As summarized in Figure 3 and Table 1, the frequencies of $\nu_{C=C}$ and $\nu_{C=N}$ for N are 1550 and 1652 cm^{-1}, respectively, and these values are very similar to those for NpSRII. However, the D_2O-induced shift of $\nu_{C=N}$ for N is −32 cm^{-1}, which is significantly larger than the corresponding shift of −21 cm^{-1} for NpSRII. This result implies that the Schiff base group experiences a stronger hydrogen bonding environment in N. A stronger hydrogen bonding in the N intermediate was also inferred from the deuteration shift for BR, i.e., the D_2O-induced shift of −17 cm^{-1} for BR changes to −24 cm^{-1} for N in BR.[24,27] A crystallographic study of BR has suggested the presence of a hydrogen-bonded chain of water molecules between the retinal Schiff base and a proton donor Asp96 in the N intermediate of BR.[32] This network of water molecules in the cytoplasmic side accounts for the strong hydrogen bond at the Schiff base C=NH moiety of N in BR. In contrast, NpSRII does not contain proton-donating groups, since Asp96 in BR corresponds to Phe86 in NpSRII. The present resonance Raman study, however, demonstrates a strong hydrogen bonding environment of the Schiff base in N, suggesting the presence of a similar network of water molecules around a Schiff base moiety.

As a possible structural model of Scheme 4, Figure 6 illustrates a proposed photocycle of NpSRII. From an analogy to BR, the reprotonation of the Schiff base in M will lead to the formation of the N intermediate that contains a 13-*cis* chromophore with a protonated Schiff base. Because of the lack of proton-donating

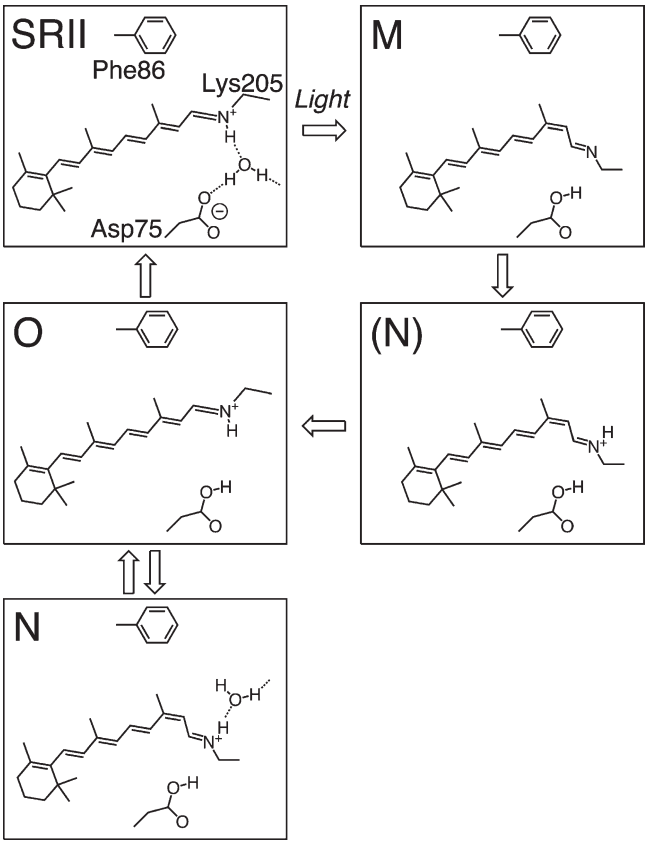

Figure 6. A proposed structural model of the photocycle for NpSRII.

groups in NpSRII, this *true* N intermediate probably does not contain a network of water molecules near the retinal Schiff base. It is therefore likely that the *true* N intermediate is unstable and immediately forms a subsequent O, since the Schiff base moiety is not stabilized by a hydrogen bond. In addition, the lack of a charged residue as a proton-donating group may also facilitate isomerization.[33−38] After the formation of O, the protein structure would change to accommodate water molecules in the cytoplasmic side. Such a protein structural change could lead to the formation of an observable N as equilibrium with O. Although the photocycle model of Figure 6 is not conclusive, it would explain both the transient absorption and resonance Raman data presented here. The molecular characterization of the protein conformation changes as well as detailed kinetic scheme will be a future investigation.

Finally, we discuss a possible biological significance of the formation N. As shown in Figure 9S in the Supporting Information, N was not detected in the transient resonance Raman spectrum of T204A. Sudo et al.[39] have shown that Thr204 is essential for signaling between NpSRII and its transducer HtrII. For instance, the T204A mutation eliminated phototaxis signaling by the NpSRII−HtrII complex. Thus the protein structural changes associated with the formation of N would be correlated with a signal relay from NpSRII to HtrII in addition to the direct interaction between retinal and opsin at earlier intermediates. Alternatively, the formation of N might be kinetically important. Since N is in equilibrium with O, the formation of N possibly contributes to a prolonged lifetime of O, which is proposed to be a signaling state.[1] The present finding also has an implication on the photocycle of SRI. Bogomolni and Spudich[40] showed that the decay process of M in SRI (also known as S373) to the initial SRI appears to occur in a concerted reaction involving the reprotonation of the Schiff base and the 13-*cis* to all-*trans* reisomerization. It is possible that this apparent first-order process also proceeds through a *true* N intermediate like NpSRII.

CONCLUSIONS

In the present study, we have examined the latter half of the photocycle in NpSRII comprised of M, N, and O by transient absorption and resonance Raman spectroscopy. These studies provide spectroscopic evidence of the presence of N during the photocycle. In addition, a global fitting analysis of the transient absorption data indicates that the reprotonation of the Schiff base in M leads to the formation of O, and N forms in equilibrium with O. Thus, the late photocycle of NpSRII is different from that of BR.[41] The transient resonance Raman spectra further demonstrate a strong hydrogen bonding environment of the protonated Schiff base in N. These observations suggest a structural model of the NpSRII photocycle, which involves entry of proton with water molecules into the cytoplasmic side of the protein.

ASSOCIATED CONTENT

Supporting Information. Supplemental results. This material is available free of charge via the Internet at http://pubs.acs.org.

AUTHOR INFORMATION

Corresponding Author

*Telephone, +81-(0)952-28-8678; fax, +81-(0)952-28-8548; e-mail, unno@cc.saga-u.ac.jp (M.U.). Telephone/fax, +81-(0)89-926-7138; e-mail, nkamo@cc.matsuyama-u.ac.jp. (N.K.).

Notes

[a]The discrepancy between the absorption maxima may be due to the small population of N. In this study, we were able to increase the fraction of N by adding azide, whereas Chizhov et al. [7] used NpSRII without azide for their experiment.

Funding Sources

This study was supported by Saga University Dean's Grant 2010 For Promising Excellent Research Projects.

ABBREVIATIONS

BR, bacteriorhodopsin; DDM, *n*-dodecyl-β-D-maltoside; SRI, sensory rhodopsin I; SRII, sensory rhodopsin II; NpSRII, SRII from *Natronobacterium pharaonis*

REFERENCES

(1) Hoff, W. D., Jung, K. H., and Spudich, J. L. (1997) Molecular mechanism of photosignaling by archaeal sensory rhodopsins. *Annu. Rev. Biophys. Biomol. Struct. 26*, 223–258.

(2) Kamo, N., Shimono, K., Iwamoto, M., and Sudo, Y. (2001) Photochemistry and Photoinduced Proton-Transfer by *Pharaonis* Phoborhodopsin. *Biochemistry (Moscow) 66*, 1277–1282.

(3) Spudich, J. L., and Luecke, H. (2002) Sensory rhodopsin II: functional insights from structure. *Curr. Opin. Struct. Biol. 12*, 540–546.

(4) Spudich, J. L., Jung, K. H. (2005) Archaeal sensory rhodopsins. In *Handbook of Photosensory Receptors* (Briggs, W. R., Spudich, J. L., Eds.) pp 1−21, Wiley VCH, Weinheim, Germany.

(5) Lanyi, J. K. (2004) Bacteriorhodopsin. *Annu. Rev. Physiol. 66*, 665–688.
(6) Miyazaki, M., Hirayama, J., Hayakawa, M., and Kamo, N. (1992) Flash photolysis study on pharaonis phoborhodopsin from a haloalkaliphilic bacterium (*Natoronobacterium pharaonis*). *Biochim. Biophys. Acta 1140*, 22–29.
(7) Chizhov, I., Schmies, G., Seidel, R., Sydor, J. R., Luttenberg, B., and Engelhard, M. (1998) The photophobic receptor from *Natronobacterium pharaonis*: Temperature and pH dependencies of the photocycle of sensory rhodopsin II. *Biophys. J. 75*, 999–1009.
(8) Iwamoto, M., Shimono, K., Sumi, M., Koyama, K., and Kamo, N. (1999) Light-induced proton uptake and release of *pharaonis* phoborhodopsin detected by a photoelectrochemical cell. *J. Phys. Chem. B 103*, 10311–10315.
(9) Iwamoto, M., Shimono, K., Sumi, M., and Kamo, N. (1999) Positioning proton-donating residues to the Schiff-base accelerates the M-decay of *pharaonis* phoborhodopsin expressed in *Escherichia coli*. *Biophys. Chem. 79*, 187–192.
(10) Furutani, Y., Iwamoto, M., Shimono, K., Kamo, N., and Kandori, H. (2002) FTIR spectroscopy of the M photointermediate in *pharaonis* phoborhodopsin. *Biophys. J. 83*, 3482–3489.
(11) Hein, M., Wegener, A. A., Engelhard, M., and Siebert, F. (2003) Time-resolved FTIR studies of sensory rhodopsin II (NpSRII) from *Natronobacterium pharaonis*: Implications for proton transport and receptor activation. *Biophys. J. 84*, 1208–1217.
(12) Takao, K., Kikukawa, T., Araiso, T., and Kamo, N. (1998) Azide accelerates the decay of M-intermediate of *pharaonis* phoborhodopsin. *Biophys. Chem. 73*, 145–153.
(13) Shimono, K., Iwamoto, M., Sumi, M., and Kamo, N. (1997) Functional expression of *pharaonis* phoborhodopsin in *Escherichia coli*. *FEBS Lett. 420*, 54–56.
(14) Sato, M., Kubo, M., Aizawa, T., Kamo, N., Kikukawa, T., Nitta, K., and Demura, M. (2005) Role of putative anion-binding sites in cytoplasmic and extracellular channels of *Natronomonas pharaonis* halorhodopsin. *Biochemistry 44*, 4775–4784.
(15) Chizhov, I., Chernavskii, D. S., Engelhard, M., Müller, K. H., Zubov, B. V., and Hess, B. (1996) Spectrally silent transitions in the bacteriorhodopsin photocycle. *Biophys. J. 71*, 2329–2345.
(16) Birge, R. R. (1990) Nature of the primary photochemical events in rhodopsin and bacteriorhodopsin. *Biochim. Biophys. Acta 1016*, 293–327.
(17) Unno, M., Kikuchi, S., and Masuda, S. (2010) Structural refinement of a key tryptophan residue in the BLUF photoreceptor AppA by ultraviolet resonance Raman spectroscopy. *Biophys. J. 98*, 1949–1956.
(18) Mathies, R. A., Smith, S. O., Palings, I. (1988) Determination of Retinal Chromophore Structure in Rhodopsins. In *Biological Applications of Raman Spectroscopy* (Spiro, T. G., Ed.) Vol. II, pp 59−108, Wiley-Interscience, New York.
(19) Ikeura, Y., Shimono, K., Iwamoto, M., Sudo, Y., and Kamo, N. (2004) Role of Arg-72 of *pharaonis* phoborhodopsin (sensory rhodopsin II) on its photochemistry. *Biophys. J. 86*, 3112–3120.
(20) Gellini, C., Lüttenberg, B., Sydor, J., Engelhard, M., and Hildebrandt, P. (2000) Resonance Raman spectroscopy of sensory rhodopsin II from *Natronobacterium pharaonis*. *FEBS Lett. 472*, 263–266.
(21) Rivas, L., Hippler-Mreyen, S., Engelhard, M., and Hildebrandt, P. (2003) Electric-field dependent decays of two spectroscopically different M-states of photosensory rhodopsin II from *Natronobacterium pharaonis*. *Biophys. J. 84*, 3864–3873.
(22) Aton, B., Doukas, A. G., Callender, R. H., Becher, B., and Ebrey, T. G. (1977) Resonance Raman studies of the purple membrane. *Biochemistry 16*, 2995–2999.
(23) Smith, S. O., Braiman, M. S., Myers, A. B., Pardoen, J. A., Courtin, J. M. L., Winkel, C., Lugtenburg, J., and Mathies, R. A. (1987) Vibrational analysis of the *all-trans*-retinal chromophore in light-adapted bacteriorhodopsin. *J. Am. Chem. Soc. 109*, 3108–3125.
(24) Althaus, T., Eisfeld, W., Lohrmann, R., and Stockburger, M. (1995) Application of Raman spectroscopy to retinal proteins. *Isr. J. Chem. 35*, 227–251.
(25) Naumann, H., Murgida, D. M., Engelhard, M., Klare, K. P., and Hildebrandt, P. (2006) Time-resolved resonance Raman spectroscopy of sensory rhodopsin II in the micro- and millisecond time range using gated cw excitation. *J. Raman Spectrosc. 37*, 436–441.
(26) Braiman, M., and Mathies, R. (1980) Resonance Raman evidence for an all-trans to 13-cis isomerization in the proton-pumping cycle of bacteriorhodopsin. *Biochemistry 19*, 5421–5428.
(27) Fodor, S. P. A., Ames, J. B., Gebhard, R., van den Berg, E. M. M., Stoeckenius, W., Lugtenburg, J., and Mathies, R. A. (1988) Chromophore structure in bacteriorhodopsin's N intermediate: Implications for the proton-pumping mechanism. *Biochemistry 27*, 7097–7101.
(28) Smith, S. O., Pardoen, J. A., Mulder, P. P. J., Curry, B., Lugtenburg, J., and Mathies, R. (1983) Chromophore structure in bacteriorhodopsin's O_{640} photointermediate. *Biochemistry 22*, 6141–6148.
(29) Iwamoto, M., Sudo, Y., Shimono, K., Araiso, T., and Kamo, N. (2005) Correlation of the O-intermediate rate with the pK_a of Asp-75 in the dark, the counterion of the Schiff base of *pharaonis* phoborhodopsin (sensory rhodopsin II). *Biophys. J. 88*, 1215–1223.
(30) Nakao, Y., Kikukawa, T., Shimono, K., Tamogami, J., Kimitsuki, N., Nara, T., Unno, M., Ihara, K., and Kamo, N. (2011) Photochemistry of a putative new class of sensory rhodopsin (SRIII) coded by xop2 of *Haloarcular marismortui*. *J. Photochem. Photobiol., B 102*, 45–54.
(31) Smith., S. O., Myers., A. B., Mathies, R. A., Pardoen, J. A., Winkel, C., van den Berg, M. M., and Lugtenburg, J. (1985) Vibrational analysis of the all-*trans* retinal protonated Schiff base. *Biophys. J. 47*, 653–664.
(32) Schobert, B., Brown, L. S., and Lanyi, J. K. (2003) Crystallographic structures of the M and N intermediates of bacteriorhodopsin: Assembly of a hydrogen-bonded chain of water molecules between Asp-96 and the retinal Schiff base. *J. Mol. Biol. 330*, 553–570.
(33) Balashov, S. P., Imasheva, E. S., Ebrey, T. G., Chen, N., Menick, D. R., and Crouch, R. K. (1997) Glutamate-194 to cysteine mutation inhibits fast light-induced proton release in bacteriorhodopsin. *Biochemistry 36*, 8671–8676.
(34) Misra, S., Govindjee, R., Ebrey, T. G., Chen, N., Ma, J.-X., and Crouch, R. K. (1997) Proton uptake and release are rate-limiting steps in the photocycle of the bacteriorhodopsin mutant E204Q. *Biochemistry 36*, 4875–4883.
(35) Dioumaev, A. K., Richter, H.-T., Brown, L. S., Tanio, M., Tuzi, S., Saito, H., Kimura, Y., Needleman, R., and Lanyi, J. K. (1998) Partitioning of free energy gain between the photoisomerized retinal and the protein in bacteriorhodopsin. *Biochemistry 37*, 2496–2506.
(36) Balashov, S. P. (2000) Protonation reactions and their coupling in bacteriorhodopsin. *Biochim. Biophys. Acta 1460*, 75–94.
(37) Dioumaev, A. K., Brown, L. S., Needleman, R., and Lanyi, J. K. (2001) Coupling of the reisomerization of the retinal, proton uptake, and reprotonation of Asp-96 in the N photointermediate of bacteriorhodopsin. *Biochemistry 40*, 11308–11317.
(38) Yamazaki, Y., Kandori, H., Needleman, R., Lanyi, J. K., and Maeda, A. (1998) Interaction of the protonated Schiff base with the peptide backbone of valine 49 and the intervening water molecule in the N photointermediate of bacteriorhodopsin. *Biochemistry 37*, 1559–1564.
(39) Sudo, Y., Furutani, Y., Kandori, H., and Spudich, J. L. (2006) Functional importance of the interhelical hydrogen bond between Thr^{204} and Tyr^{174} of sensory rhodopsin II and its alteration during the signaling process. *J. Biol. Chem. 281*, 34239–34245.
(40) Bogomolni, R. A., and Spudich, J. L. (1987) The photochemical reactions of bacterial sensory rhodopsin-I. Flash photolysis study in the one microsecond to eight second time window. *Biophys. J. 42*, 1071–1075.
(41) Kikukawa, T., Saha, C. K., Balashov, S. P., Imasheva, E. S., Zaslavsky, D., Gennis, R. B., Abe, T., and Kamo, N. (2008) The lifetimes of *pharaonis* phoborhodopsin signaling states depend on the rates of proton transfers—effects of hydrostatic pressure and stopped flow experiments. *Photochem. Photobiol. 84*, 880–888.